Minerals Engineering 145 (2020) 106076

Contents lists available at ScienceDirect

Minerals Engineering

journal homepage: www.elsevier.com/locate/mineng

Leaching efficiency of sulfuric acid on selective lithium leachability from bauxitic claystone

Hannian Gu[a,c,*], Tengfei Guo[a,c], Hanjie Wen[b,c,*], Chongguang Luo[b], Yi Cui[b], Shengjiang Du[b], Ning Wang[a]

[a] Key Laboratory of High-temperature and High-pressure Study of the Earth's Interior, Institute of Geochemistry, Chinese Academy of Sciences, Guiyang 550081, China
[b] State Key Laboratory of Ore Deposit Geochemistry, Institute of Geochemistry, Chinese Academy of Sciences, Guiyang 550081, China
[c] University of Chinese Academy of Sciences, Beijing 100049, China

ARTICLE INFO

Keywords:
Lithium
Bauxitic clay
Leaching behavior
Calcination
Montmorillonite

ABSTRACT

The explosive demand for lithium calls for new lithium resources. A lithium-rich bauxitic clay was selected, and its material composition, phase transformation, lithium leaching efficiency using sulfuric acid were investigated after calcination treatment. In this study, XRF, ICP-AES, ICP-MS, XRD and SEM were employed to characterize bauxitic clay and its calcining products and leaching residues. The results show that bauxitic clay mainly consists of diaspore, illite, montmorillonite and anatase with a major chemical composition of Al_2O_3 (48.01%), SiO_2 (33.06%), K_2O (3.88%), TiO_2 (2.25%), Fe_2O_3 (1.07%), MgO (0.46%), and lithium 3170 μg/g. The optimum calcination temperatures were 500 and 600 °C, with 72.34% and 73.61% lithium extracted, respectively, using 15% sulfuric acid leaching for 1 h. The optimal leaching conditions for lithium extraction were a leaching reaction time of 60 min and a 20% (wt/v) sulfuric acid concentration. Lithium leaching in this study was considered to occur via ion exchange instead of mineral dissolution. The findings of this study would be useful and interesting for lithium recovery from bauxitic clay.

1. Introduction

Lithium (Li) resources are crucial raw materials for various industrial demands, and lithium compounds are used in a wide range of applications (Zhang et al., 2017; Ryu et al., 2019). In recent years, the consumption of lithium has increased rapidly because of its substantial demand in lithium-ion batteries, for example, in mobile phones, in laptops, and especially in automotive batteries for electric vehicles (Meshram et al., 2014; Swain, 2017; Zhang et al., 2017; Shi et al., 2018). The explosive demand for lithium for its various applications places significant pressure on lithium resources (Meshram et al., 2014). Lithium is traditionally produced from a variety of natural sources, such as minerals (e.g., spodumene and lepidolite), salt lakes, and underground brine reservoirs. Natural lithium resources are simply defined as two broad categories, namely, rock sources and brine sources (Mohr et al., 2012; Tadesse et al., 2019). In addition, some sedimentary clays containing hectorite have also been developed as lithium sources (Meshram et al., 2014). However, as a minor component of igneous rocks, lithium in minerals (primarily in pegmatite) is distinguished from clay type resource owing to their different geologic environments (Kesler et al., 2012). Mineral lithium and brine lithium are economic sources of lithium and have been successively exploited (Mohr et al., 2012). Despite their large potential size, few reports have referred to exploiting clay type lithium resources. Due to the depletion of lithium ores and the high cost of solvents for lithium separation from salt lake brine, lithium-bearing clays have received increasing attention (Benson et al., 2017).

Among the sedimentary clay type of lithium resources, the jadarite-type and hectorite-type deposits are widely known. Jadarite is a kind of lithium-boron-containing mineral found in the Jadar lithium deposit, Serbia, which has been estimated to be a resource of lithium averaging 1.4% lithium (Kesler et al., 2012; Mohr et al., 2012). The Kings Valley lithium deposit in Nevada consists of layers of the lithium-bearing smectite clay hectorite, and its origin is similar to that of the original hectorite discovery at the Hector mine near Barstow, California. The lithium content of hectorite-type deposits is usually much lower than that of jadarite-type deposits (Kesler et al., 2012). However, current evidence suggests that jadarite-type lithium deposit is not as common as hectorite-type lithium deposit. Hectorite-type lithium deposits have a wide distribution, e.g., Egyptian montmorillonite-type clay (bentonite clay) was also reported to contain as high as 1.2% Li_2O, and lithium occurs as hectorite in the clay samples (Amer, 2008). A lithium-bearing

* Corresponding authors.
E-mail addresses: guhannian@vip.gyig.ac.cn (H. Gu), wenhanjie@vip.gyig.ac.cn (H. Wen).

https://doi.org/10.1016/j.mineng.2019.106076
Received 4 July 2019; Received in revised form 4 October 2019; Accepted 8 October 2019
Available online 25 October 2019
0892-6875/

smectite from Kings Mountain, North Carolina is known as swinefordite, with the highest lithium content known in clays ranging from 4.29 to 5.66 wt% Li_2O (Tadesse et al., 2019). In addition to being large scale, the sedimentary clay types of lithium resources have relatively simple compositions that will free them from processing and by-product complications (Kesler et al., 2012). In China, many Karst-type bauxite deposits are enriched in lithium, which was reported as hosting within the Li-bearing claystone (Liu et al., 2013; Wang et al., 2013; Ling et al., 2018). Karst-type bauxite contains diaspore and/or boehmite as the main aluminum-rich mineral (Ling et al., 2015), and clay minerals in Karst-type bauxite account for a high volume compared to other types of bauxite. The lithium concentrations in clay rocks with an average of 425.5 μg/g were higher than those in bauxite ores (average of 306.5 μg/g) (Ling et al., 2018). The high concentration was attributed to the affinity of lithium to aluminosilicates (especially clay minerals). Clay rocks around bauxite ore (also called bauxitic clay/claystone) usually contain more clay minerals than bauxite ores; thus, they contain a higher content of lithium. Therefore, these bauxitic claystones can also be considered one of the sedimentary clay/clay-related types of lithium resources.

Attempts to recover lithium from the lithium-bearing clays are mainly restricted to a few earlier studies (Amer, 2008). After a large deposit of lithium-bearing clay on the Nevada-Oregon border was identified, many extraction techniques were proposed by researchers from the US Bureau of Mines (Crocker and Lien, 1987). The lithium concentration in the clay was 0.1 to 0.64%, and a typical clay sample containing 0.6% lithium was used for extraction tests. After roasting at 900 °C, a mixture of clay and limestone - gypsum can be leached using water, and up to approximately 90% lithium entered into the solution (Lien, 1985). Another roast-leach process was reported by Crocker and Lien (1987), obtaining a recovery of > 85% lithium by roasting montmorillonite-type clays (0.3–0.6%, Li) with KCl-$CaSO_4$, followed by water leaching. Crocker and Lien (1987) also reported a process for lithium extraction by chlorination of hectorite in clays with limestone at 750 °C using 20 wt% HCl. A hydrometallurgical extraction method using H_2SO_4 for processing El-Fayoum bentonites at 250 °C was demonstrated to effectively leach > 90% lithium under favorable conditions (Amer, 2008). In most cases, calcination treatment is necessary for freeing lithium from lithium-bearing mineral in clays followed by leaching.

In the current study, a kind of lithium-rich bauxitic clay was characterized, and the leaching efficiency of lithium from calcined clays without additives was investigated. The leaching mechanism of lithium from the bauxitic clay was also preliminarily discussed. Knowledge of the leaching behavior of lithium from bauxitic claystone would be useful for lithium recovery and purification for further processing.

2. Materials and methods

2.1. Raw materials and characterization methods

The bauxitic claystone used in this study was collected from Jinsha County, Northwest Guizhou, China. The claystone was crushed and ground into fine powder using a mortar and pestle and was then dried and homogenized for the characterization and leaching experiments. Before the leaching process, the bauxitic claystone was calcined at different temperatures under air conditions.

The main chemical compositions of the bauxitic claystone were determined using X-Ray Fluorescence Spectroscopy (XRF, PANalytical PW2424). The XRF analysis was conducted in conjunction with a loss-on-ignition (LOI) method at 1000 °C. The trace elemental compositions of the sample were analyzed by inductively coupled plasma-atomic emission spectrometry (ICP-AES, Agilent VISTA) or inductively coupled plasma-mass spectrometry (ICP-MS, Agilent 7700x). A prepared sample was digested with perchloric, nitric and hydrofluoric acids, and the residue was leached with dilute hydrochloric acid and diluted to volume. Finally, the solution was then analyzed by ICP-AES or ICP-MS.

Bauxitic claystone and samples calcined at different temperatures were characterized by powder X-ray diffraction (XRD) with measurements performed using a PANalytical Empyrean diffractometer with Cu Kα radiation. Each sample was prepared by compaction into a silicon sample holder, and a 2θ range between 5 and 70 deg was scanned. Samples for scanning electron microscopy (SEM) observation were viewed in an FEI Scios scanning electron microscope.

2.2. Leaching process

Bauxitic claystone in this study was calcined using a muffle furnace at different temperatures (300, 400, 500, 600, 700, 800 and 900 °C) for 1 h. The calcined products were then leached by sulfuric acid under different conditions. The calcined samples at each temperature were leached with 15 wt/v % H_2SO_4 at 20, 40, 60 and 80 °C for 1 h; this process was conducted and monitored by an electric heater/thermostatic water bath. In contrast, the raw sample dried at 105 °C without calcining treatment was also leached. In addition, the efficiencies of the acid amount and leaching time on the lithium leaching were studied to confirm the optimal conditions in this study. For the acid amount trials, leaching reactions using different acid concentrations (2.5, 5, 15, 20 and 25 wt/v % H_2SO_4) were performed for 1 h with a solid:solution ratio of 3.0 g/15 mL at 80 °C with constant gentle agitation. For leaching time trials, leaching reactions using 15 wt/v % H_2SO_4 were performed from 10 min to 5 h with a solid:solution ratio of 3.0 g/15 mL at 80 °C with constant gentle agitation.

The sulfuric acid used in the leaching process was guaranteed reagent (GR) grade. The element concentrations in the leaching solutions were determined by ICP-OES (Varian VISTA). From the above analysis, the percentage extraction of lithium (or other metals) was calculated according to the following equation (1):

$$\varepsilon(\mathrm{M}, \%) = \frac{V * c}{m * w} \times 100 \quad (1)$$

where ε (M, %) represents the leaching ratio of Li, Al, Fe, or Mg; V (L) is the total volume of the acid leaching solution merged with the washing solution; c (g/L) is the concentration of Li, Al, Fe, or Mg in the solution; m (g) is the weight of the raw bauxitic clay used; and w (%) is the content of Li, Al, Fe, or Mg in the bauxitic clay sample.

3. Results and discussion

3.1. Chemical and mineral composition

Table 1 shows that Al_2O_3 and SiO_2 were the major chemical constituents in the bauxitic claystone sample followed by K_2O, TiO_2, Fe_2O_3, MgO, P, S, etc. In economic geology, industrial-grade bauxite refers specifically to deposits containing > 35% Al_2O_3 and a weight ratio of Al_2O_3:SiO_2 > 2.6 (Yu et al., 2019). In this study, the content of Al_2O_3 (48.01%) is higher than 35%, and the weight ratio of Al_2O_3:SiO_2 is only 1.45, which is less than the industrial requirements. Therefore, it is a

Table 1
Main chemical compositions of the bauxitic clay sample in this study.

Components	Al_2O_3	SiO_2	Fe_2O_3	TiO_2	K_2O	CaO	Na_2O	MgO	P_2O_5	SO_3	LOI
wt %	48.01	33.06	1.07	2.25	3.88	0.03	0.09	0.46	0.12	0.04	10.42

Table 2
Trace elemental concentrations of the bauxitic clay sample in this study.

Elements	Li	Ba	Cr	Ce	La	Nb	Ni	Pb	Sc	Sn	Sr	Ta	V
μg/g	3170	120	135	41.4	14.6	41.2	85.3	49.1	53.4	9.7	285	3.23	150

bauxitic clay/claystone instead of bauxite ore. In the bauxitic claystone, K_2O is higher than most of the bauxite ore bodies or wall rocks (Zhang et al., 2013; Ling et al., 2015; Yu et al., 2019), which can be explained by a high content of illite inside of the bauxitic claystone. Other compositions, such as CaO, Na_2O, and MgO, are all no more than 0.5%, and the LOI is attributed to the dehydration of the hydrous aluminum silicate minerals.

The trace elemental compositions inclusive of lithium are listed in Table 2. As seen in Table 2, the concentration of lithium in the bauxitic clay is as high as 3170 μg/g. Wang et al. (2013) discovered that lithium was as high as 2715.60 μg/g in the Dazhuyuan bauxite deposit, and Cui et al. (2018) reported that bauxitic clay contained averaging 980 μg/g lithium (with the highest concentration reaching 3453 μg/g). In most cases, a high content of lithium could be found in the bauxitic clay, which contained higher clay minerals than bauxite ore. Rare earth elements (such as La and Ce) and rare metals (Nb and Ta) in the bauxitic clay sample, as shown in Table 2, are low and have no economic interest.

XRD analysis of the bauxitic claystone identifies the mineral phase composition -diaspore, illite, montmorillonite and anatase (Fig. 1). With respect to the absence of crystalline iron minerals in the sample, iron is most likely in the form of isomorphism phases or as a minor component that is too minute to be determined. Fig. 1 also presents the converted products obtained by calcining bauxitic claystone samples at various temperatures. From 500 °C onward, the peaks of diaspore and montmorillonite disappeared, converting to aluminum oxide and dehydrated montmorillonite, respectively.

3.2. Influence of the calcination temperature for metal leaching

Fig. 2 shows the leaching behaviors of metals from raw bauxitic claystone and its converted products calcined at different temperatures. The results show that for the four investigated metals (Li, Al, Fe and Mg), their leaching ratios did not exceed 16% based on bauxitic claystone samples without calcination and calcined at 300 and 400 °C (Fig. 2a–c). This finding suggests that the dissolution of metals is incomplete when sulfuric acid is used to leach these samples. The iron leaching ratio increases slightly with increasing leaching temperature,

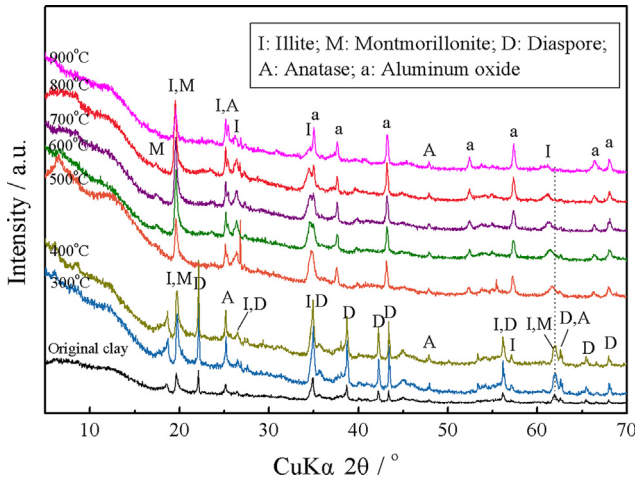

Fig. 1. XRD patterns of the raw bauxitic clay and its calcining products at different temperatures.

while the change curves of lithium, aluminum and magnesium do not obviously change with increasing leaching temperature. In the bauxitic claystone samples calcined at 500 and 600 °C (Fig. 2d,e), the lithium and magnesium leaching rates increase dramatically at different leaching temperatures, and as the leaching temperature arrives at 80 °C, the maximal leaching efficiency of lithium reaches 72.34% and 73.61%, respectively. As a whole, based on the samples calcined at 500, 600, 700 and 800 °C, metal leaching rates demonstrate an apparent increase with increasing leaching temperature (Fig. 2d–g), indicating that leaching temperature plays an important role in the leaching process. When the calcination temperatures are set at 700 and 800 °C, the metal leaching rates from the calcined bauxitic claystone samples exhibit a declining trend at each reaction temperature. As the heating temperature further increased to 900 °C, the leaching rates of all four investigated metals severely decreased to less than 8.3% (Fig. 2h).

According to previous literature with respect to the structural transformation of clay minerals (Chen et al., 2017), we hypothesize that three stages are experienced during the heating process: dehydration before 500 °C, a gradual collapse of the layer structure from 500 to 800 °C, and structure destroy and/or new phase formation from 900 °C. Before 500 °C, clay minerals (e.g., montmorillonite) are subjected to the loss of adsorbed water and the dehydration of hydrated cations, and their stratified structures remain. This process can explain the fact that the leaching rates of lithium increase slightly from raw bauxitic clay to its products calcined at 300 and 400 °C. In the range of approximately 500 to 800 °C (Buchwald et al., 2009), structural hydroxyl groups release, and the layers of clay minerals begin to collapse, which causes the space between layers to change and leads the interlayer cation to be exchangeable. However, dehydroxylation occurs depending on the calcination temperature for the different types of clay minerals (Taylor-Lange et al., 2014; Stevenson and Gurnick, 2016). Moreover, as the calcination temperature increases, the interlayer cation may be covered or retightened. This behavior can explain that lithium (exclusive in the crystal lattice if any) in the clay layers dissolves at high levels at 500 and 600 °C, with a moderate decline from 600 and 800 °C. At temperatures greater than 900 °C, the clay minerals (e.g., montmorillonite) form various firing products depending upon their structures (Stevenson and Gurnick, 2016). The firing products, such as cordierite and spinel, solidify the metals from leaching by the solution.

The leaching trends observed from the curves in Fig. 2 show that lithium and magnesium are leached exclusively from the same mineral phases, i.e., clay minerals. Octahedral Al in montmorillonite is partially substituted by Mg (Marchel and Stanjek, 2012; Etcheverry et al., 2017), and montmorillonite is considered the source of Mg in the bauxitic clay in this study. As shown in Fig. 2, lithium has a higher leaching rate than magnesium under the same conditions, suggesting that the amount of lithium that can be dissolved in the acid leaching process is larger than that of magnesium for the calcined samples. Lithium is mainly in the clay structure layers, while magnesium presents as Mg-O octahedra, which may explain why lithium has a higher leaching rate than magnesium. The interlayer of potassium in illite inhibits water molecules inside (Stevenson and Gurnick, 2016). High temperature reaction can free lithium from the silicate by a variety of ion substitution or ion exchange (Colton, 1957; White and McVay, 1958). In lithium refineries, ion substitution or ion exchange of H^+ for Li^+ happens during the subsequent digestion of β-spodumene (transformed from α-spodumene after high temperature) with concentrated sulfuric acid (Abdullah et al., 2019). Due to the small interlayer space, illite has a much lower cation exchange capacity than montmorillonite (Alastair et al., 2018). In

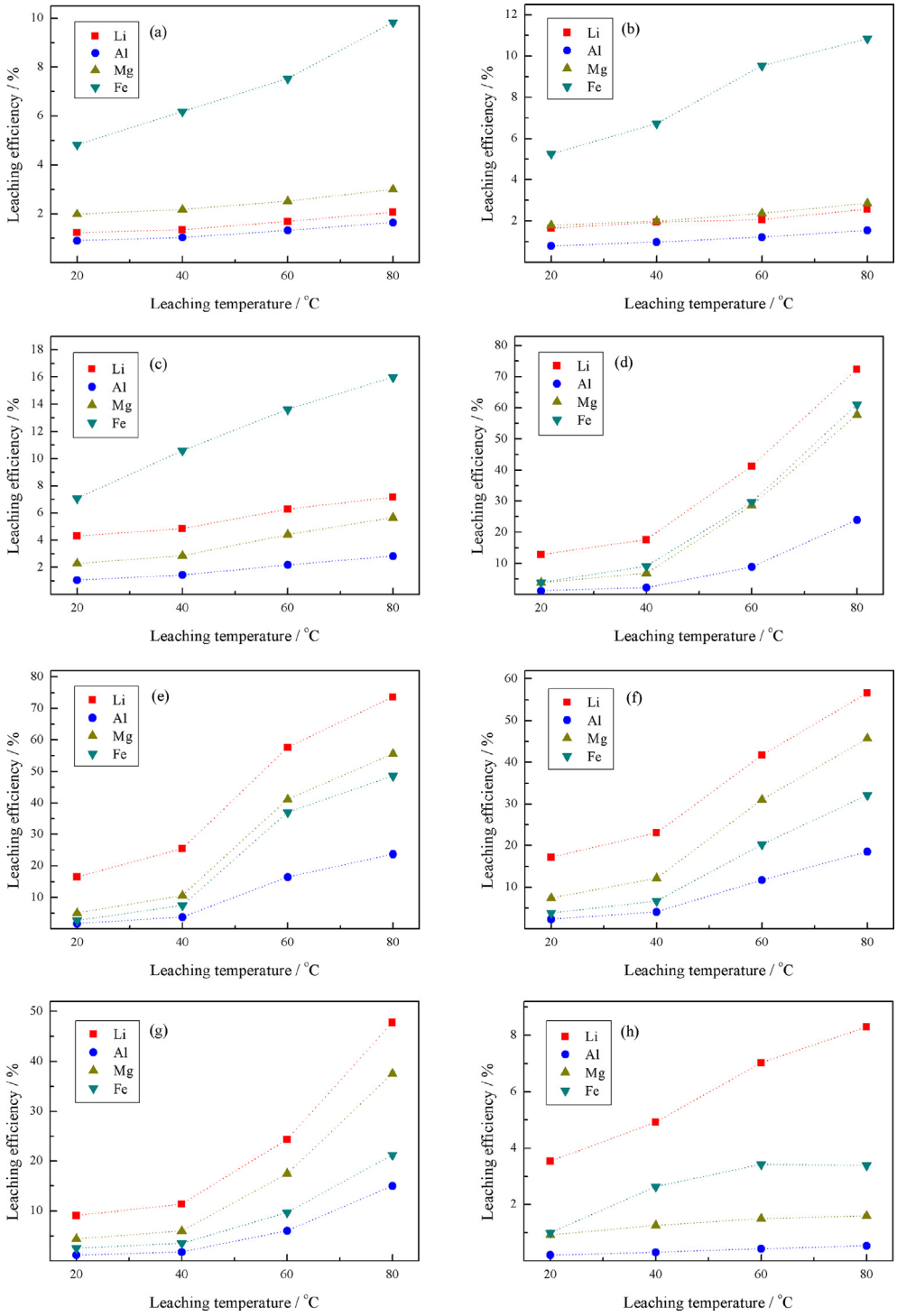

Fig. 2. Metal leaching efficiency of raw bauxitic clay (a), and the influence of the calcination temperature: 300 °C, (b); 400 °C, (c); 500 °C, (d); 600 °C, (e); 700 °C, (f); 800 °C, (g); 900 °C, (h).

comparison to montmorillonite, illite experiences a less structural collapse when subjected to a high calcination temperature. This finding may explain why the leaching rate of potassium is low for all calcined samples (see Supporting information).

Iron in clays usually presents as oxides or hydroxides and can be dissolved by mineral acids at room temperature or under heating conditions (Wang et al., 2018). However, iron content in the claystone in this study is approximately 1% (Fe_2O_3), and the majority of iron is probably isomorphic with Al, similar to Mg in the minerals. The leaching iron from oxides or hydroxides contributes the high leaching rates from samples calcined before 500 °C (Fig. 2a–c), and explains why iron has higher leaching rates than magnesium, as illustrated in Fig. 2h.

As discussed above, the primary sources of aluminum in the raw bauxitic clay sample and calcined samples are from diaspore (aluminum oxide), illite and montmorillonite (dehydroxylated clays). The highest two leaching rates of aluminum were 23.92% and 23.66%, from the samples calcined at 500 and 600 °C, respectively. These results suggest that the dissolution of aluminum is incomplete, and the dominant phase of aluminum oxide is dissolved partly in the acid solution. Aluminum oxide (transformed from diaspore) contributes the most

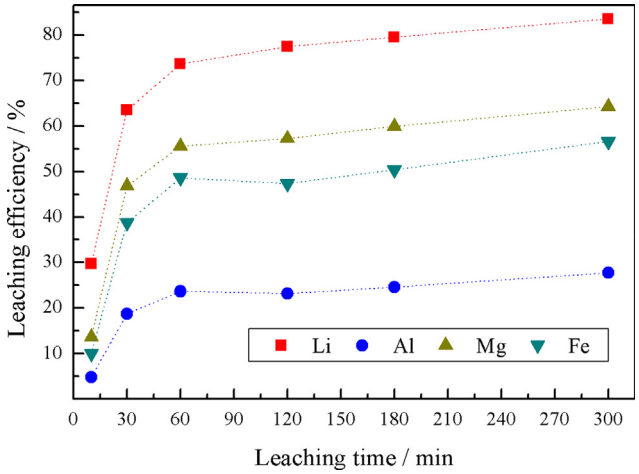

Fig. 3. Effect of the leaching time on the leaching efficiency of Li, Al, Fe and Mg from bauxitic clay calcined at 600 °C for 1 h at a leaching condition of using 15 wt/vol % H_2SO_4 at 80 °C with a liquid-solid ratio of 5:1 mL/g.

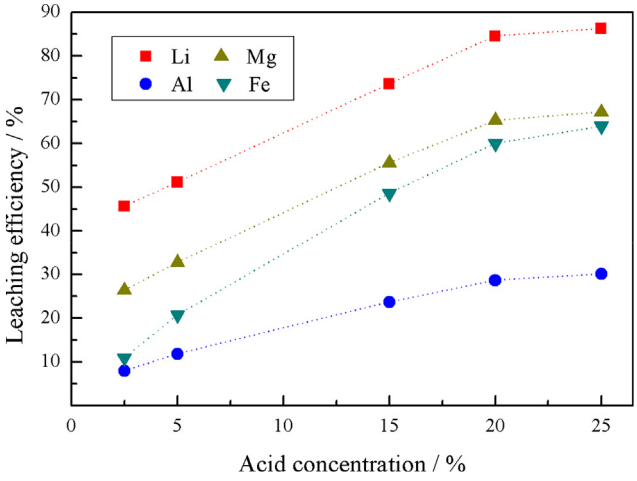

Fig. 4. Effect of the acid amount on the leaching efficiency of Li, Al, Fe and Mg from bauxitic clay calcined at 600 °C for 1 h at a leaching condition of 80 °C for 60 min with a liquid-solid ratio of 5:1 mL/g.

amount of dissolved Al, and the rate of releasing Al from dehydroxylated illite is probably lower than dehydroxylated montmorillonite because illite has less Al-O octahedra substituted by Mg in its sandwich structure (Stevenson and Gurnick, 2016). Aluminum from dehydroxylated montmorillonite (Al-O octahedra) partially dissolves for its in-depth collapse and isomorphism substitution of Mg and Fe. The highest leaching rate of Si with 3.65% (see Supporting information), implies that silicates (Si-O tetrahedra), including montmorillonite and illite, are not dissolved. Thus, it is difficult to compare the degree of dissolved aluminum from the above sources of aluminum-containing minerals, especially from dehydroxylated montmorillonite. The low leaching rates of aluminum will be conducive to the separation and purification of lithium products in the subsequent process.

3.3. The effect of the reaction time on metal leaching

The bauxitic clay samples calcined at 600 °C were leached in 15% sulfuric acid at 80 °C with a liquid-solid ratio of 5:1 mL/g. Fig. 3 shows the variation in metal leaching with reaction time. Trends in metal leaching with regard to reaction time show an apparent increase in the first 60 min and then a slow increase until the maximum duration studied. The leaching of lithium exceeds 73.61% when leached for over 60 min, and it reaches 83.49% as the leaching time is further extended to 300 min. The leaching of magnesium and iron are less than 65% and 57%, respectively. Over the entire time period studied, aluminum presents the lowest leaching rates, no higher than 28%. Therefore, the suitable leaching time for lithium extraction in this study is suggested as 60 min.

3.4. The effect of acid concentration on metal leaching

The bauxitic claystone samples calcined at 600 °C were leached with different sulfuric acid concentrations at 80 °C for 60 min with a liquid-solid ratio of 5:1 mL/g. As shown in Fig. 4, the leaching of metals increases with increasing sulfuric acid concentration. The leaching rate of lithium reaches 86.23% when the sulfuric acid concentration is 25%. Aluminum, iron and magnesium have similar leaching trendlines with lithium, and their leaching rates are lower than lithium. When the acid concentration rises to 25% from 20%, the increment in lithium is less than 2%. It is suggested that the amount of 20% sulfuric acid is the optimal condition. Magnesium is a concomitant metal for subsequent lithium separation (Shi et al., 2018). However, in this study, the leaching rates of magnesium are lower than those of lithium under different leaching conditions. In the bauxitic clay used in the current study, the content of lithium is higher than that of magnesium, implying that a solution with a high Li/Mg ratio would be obtained after the sulfuric acid leaching process. The selective leaching process is thought to be beneficial for of lithium extraction and subsequent separation and purification.

3.5. Characterization of the leaching residue

Montmorillonite in bauxitic claystone is believed to be one of the host phases of lithium. Clay minerals, including illite and montmorillonite, can dehydroxylate easily because the heating temperature is in the range of 400–800 °C (Fernandez et al., 2011). In the acid leaching process, lithium can be leached from the calcined samples in this study, indicating that dehydrated montmorillonite is highly active for releasing lithium.

Fig. 5 shows the raw bauxitic claystone, the bauxitic claystone calcined at 500 °C and the leaching residues after acid leaching at various temperatures. Residues with different efficiencies of leached metals have similar phase compositions (Fig. 5), implying that the main mineral phases do not decompose when lithium was extracted. It has been reported that illite and montmorillonite appear to conserve the order of their structural layers, even after complete dehydroxylation

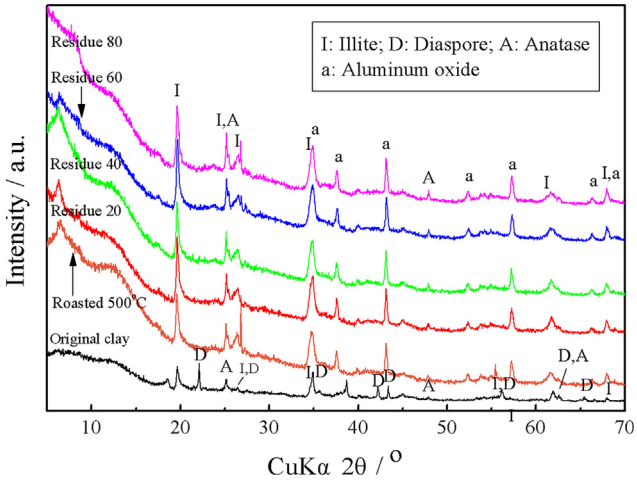

Fig. 5. XRD patterns of the raw bauxitic clay, the bauxitic clay calcined at 500 °C and the leaching residues after the acid leaching process at reaction temperatures of 20 °C (Residue 20), 40 °C (Residue 40), 60 °C (Residue 60) and 80 °C (Residue 80).

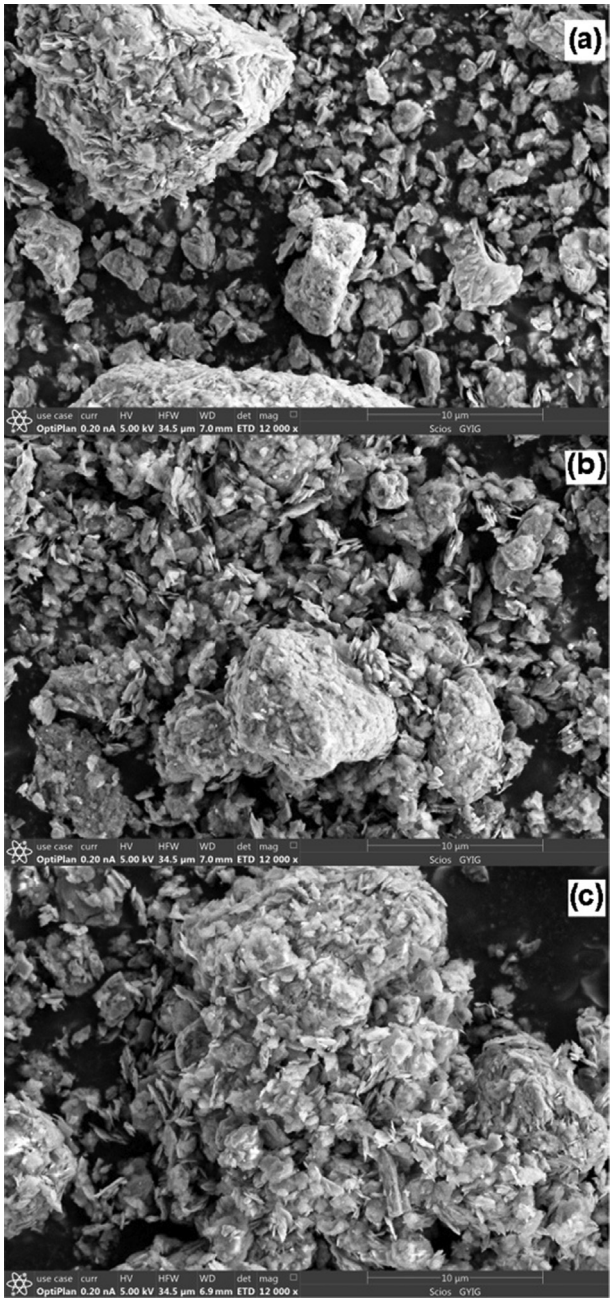

Fig. 6. SEM images of raw bauxitic clay (a), bauxitic clay calcined at 500 °C (b), and its leaching residue after the acid leaching process under optimal conditions (c).

(Fernandez et al., 2011). In this study, the SEM images before and after the leaching process at optimal conditions, as shown in Fig. 6, confirm that the stratified structures of clay minerals were not destroyed. Therefore, it is believed that lithium is leached into the solution via ion exchange instead of mineral dissolution. The interlayer spacing of clay minerals is compacted along with the interlayer/adsorbed water losing, and the structural collapse happens in clay minerals, serving to release lithium together with dehydroxylation, and smaller ions (hydrion) enter. This behavior may be considered a special ion exchange process. On the other hand, the remaining stratified structures of clay minerals (shown in Fig. 6) demonstrate that clay minerals do not dissolve during the acid leaching process.

4. Conclusions

The lithium-rich bauxitic clay investigated in this study contains 3170 μg/g lithium, and the major chemical compositions were Al_2O_3 (48.01%), SiO_2 (33.06%), K_2O (3.88%), TiO_2 (2.25%), Fe_2O_3 (1.07%), MgO (0.46%), etc. Diaspore, illite, montmorillonite and anatase occurred as the main mineral phases in the bauxitic clay.

The raw and calcined samples were leached using sulfuric acid under different conditions. The results show that calcination can effectively increase the release capacity of lithium into the solution, while higher calcination temperatures on samples decreased the leaching efficiency of lithium. At calcination temperatures of 500 and 600 °C, 72.34% and 73.61%, respectively, of lithium can be extracted using 15% sulfuric acid leaching for 1 h. In addition, lithium always exhibited higher leaching efficiencies than iron, aluminum or magnesium, suggesting that sulfuric acid was selective for leaching lithium. In this study, the optimal leaching conditions for lithium extraction were a leaching reaction time of 60 min, a 20% sulfuric acid concentration. From the XRD and SEM analyses of calcined bauxitic clay and the leached residues, lithium was suggested to be leached by ion exchange instead of mineral dissolution.

Declaration of Competing Interest

The authors declare that they have no known competing financial interests or personal relationships that could have appeared to influence the work reported in this paper.

Acknowledgements

The authors would like to acknowledge the financial supports from the National Key Research and Development Program of China (2017YFC0602503), the National Natural Science Foundation of China (Grant No. 41972048; U1812402), the Guizhou Provincial Science and Technology Foundation([2016]1155), and the Guizhou Scientific and Technological Innovation Team (2017-5657).

Appendix A. Supplementary material

Supplementary data to this article can be found online at https://doi.org/10.1016/j.mineng.2019.106076.

References

Abdullah, A.A., Oskierski, H.C., Altarawneh, M., Senanayake, G., Lumpkin, G., Dlugogorski, B.Z., 2019. Phase transformation mechanism of spodumene during its calcination. Miner. Eng. 140, 105883.
Alastair, M., Andrew, H., Pascaline, P., Mark, E., Pete, W., 2018. Alkali activation behaviour of un-calcined montmorillonite and illite clay minerals. Appl. Clay Sci. 166, 250–261.
Amer, A.M., 2008. The hydrometallurgical extraction of lithium from Egyptian Montmorillonite-Type clay. JOM 60 (10), 55–57.
Benson, T.R., Coble, M.A., Rytuba, J.J., Mahood, G.A., 2017. Lithium enrichment in intracontinental rhyolite magmas leads to Li deposits in caldera basins. Nat. Commun. 8, 270.
Buchwald, A., Hohmann, M., Posern, K., Brendler, E., 2009. The suitability of thermally activated illite/smectite clay as raw material for geopolymer binders. Appl. Clay Sci. 46, 300–304.
Chen, Q., Zhu, R., Ma, L., Zhou, Q., Zhu, J., He, H., 2017. Influence of interlayer species on the thermal characteristics of montmorillonite. Appl. Clay Sci. 135, 129–135.
Colton, J.W., 1957. Recovery of lithium from complex silicates. Advances in Chemistry, Handling and Uses of The Alkali Metals. Chapter 1, vol. 19, pp. 3–8.
Crocker L., Lien R.H., 1987. Lithium and its recovery from low-grade Nevada clays. Bulletin 691. US Bureau of Mines, Department of Interior, 1–37.
Cui, Y., Luo, C., Xu, L., Zhang, H., Deng, M., Gu, H., Meng, Y., Qin, C., Wen, H., 2018. Weathering origin and enrichment of lithium in clay rocks of the Jiujialu Formation, central Guizhou Province, Southwest China. Bull. Mineral. Petrol. Geochem. 37 (4), 696–704 (In Chinese).
Etcheverry, M., Cappa, V., Trelles, J., Zanini, G., 2017. Montmorillonite-alginate beads: natural mineral and biopolymers based sorbent of paraquat herbicides. J. Environ. Chem. Eng. 5, 5868–5875.
Fernandez, R., Martirena, F., Scrivener, K.L., 2011. The origin of the pozzolanic activity of

calcined clay minerals: a comparison between kaolinite, illite and montmorillonite. Cem. Concr. Res. 41, 113–122.
Kesler, S.E., Gruber, P.W., Medina, P.A., Keoleian, G.A., Everson, M.P., Wallington, T.J., 2012. Global lithium resources: relative importance of pegmatite, brine and other deposits. Ore Geol. Rev. 48, 55–69.
Lien, R.H., 1985. Recovery of lithium from a Montmorillonite-Type clay. Bur. Mines Rep. Invest. 8967, 1–26.
Ling, K., Zhu, Z., Tang, H., Wang, Z., Yan, H., Han, T., Chen, W., 2015. Mineralogical characteristics of the karstic bauxite deposits in the Xiuwen ore belt, Central Guizhou Province, Southwest China. Ore Geol. Rev. 65, 84–96.
Ling, K., Zhu, Z., Tang, H., Du, S., Gu, J., 2018. Geology and geochemistry of the Xiaoshanba bauxite deposit, Central Guizhou Province, SW China: implications for the behavior of trace and rare earth elements. J. Geochem. Explor. 190, 170–186.
Liu, X., Wang, Q., Feng, Y., Li, Z., Cai, S., 2013. Genesis of the Guangou karstic bauxite deposit in western Henan, China. Ore Geol. Rev. 55, 162–175.
Marchel, C., Stanjek, H., 2012. Cation ordering in cis-and trans-vacant dioctahedral smectites and its implications for growth mechanisms. Clay Miner. 47, 105–115.
Meshram, P., Pandey, B.D., Mankhand, T.R., 2014. Extraction of lithium from primary and secondary sources by pre-treatment, leaching and separation: a comprehensive review. Hydrometallurgy 150, 192–208.
Mohr, S.H., Mudd, G.M., Giurco, D., 2012. Lithium resources and production: critical assessment and global projections. Minerals 2, 65–84.
Ryu, T., Shin, J., Ghoreishian, S.M., Chung, K.-S., Huh, Y.S., 2019. Recovery of lithium in seawater using a titanium intercalated lithium manganese oxide composite. Hydrometallurgy 184, 22–28.
Shi, D., Zhang, L., Peng, X., Li, L., Song, F., Nie, F., Ji, L., Zhang, Y., 2018. Extraction of lithium from salt lake brine containing boron using multistage centrifuge extractors. Desalination 441, 44–51.
Stevenson, C.M., Gurnick, M., 2016. Structural collapse in kaolinite, montmorillonite and illite clay and its role in the ceramic rehydroxylation dating of low-fired earthenware. J. Archaeol. Sci. 69, 54–63.
Swain, B., 2017. Recovery and recycling of lithium: a review. Sep. Purif. Technol. 172, 388–403.
Tadesse, B., Makuei, F., Albijanic, B., Dyer, L., 2019. The beneficiation of lithium minerals from hard rock ores: a review. Miner. Eng. 131, 170–184.
Taylor-Lange, S.C., Rajabali, F., Holsomback, N.A., Riding, K., Juenger, M.C.G., 2014. The effect of zinc oxide additions on the performance of calcined sodium montmorillonite and illite shale supplementary cementitious materials. Cem. Concr. Compos. 53, 127–135.
Wang, D., Li, P., Qu, W., Yin, L., Zhao, Z., Lei, Z., Wen, S., 2013. Discovery and preliminary study of the high tungsten and lithium contents in the Dazhuyuan bauxite deposit, Guizhou, China. Sci. China Earth Sci. 56 (1), 145–152.
Wang, N., Gu, H., Wen, H., Liu, S., 2018. Enrichment of niobium and titanium from kaolin using an acid-alkali leaching process. Metall. Mater. Trans. B 49 (6), 3552–3558.
White, G., McVay, T.N., 1958. Some Aspects of the Recovery of Lithium from Spodumene (No. ORNL-2450). Oak Ridge. National Lab., Tenn.
Yu, W., Algeo, T.J., Yan, J., Yang, J., Du, Y., Huang, X., Weng, S., 2019. Climatic and hydrologic controls on upper Paleozoic bauxite deposits in South China. Earth Sci. Rev. 189, 159–176.
Zhang, L., Li, L., Shi, D., Li, J., Peng, X., Nie, F., 2017. Selective extraction of lithium from alkaline brine using HBTA-TOPO synergistic extraction system. Sep. Purif. Technol. 188, 167–173.
Zhang, Z., Zhou, L., Li, Y., Wu, C., Zheng, C., 2013. The “coal–bauxite–iron” structure in the ore-bearing rock series as a prospecting indicator for southeastern Guizhou bauxite mines. Ore Geol. Rev. 53, 145–158.